DISPERSION OF SMALL HEAVY PARTICLES IN A UNIFORMLY SHEARED TURBULENCE

Mitsuru Tanaka[1], Tsuyoshi Miyagawa[2]
Yasushi Maeda[1] and Yoshimichi Hagiwara[1]

[1] Department of Mechanical and System Engineering, Kyoto Institute of Technology
Sakyo-ku, Kyoto-shi, Kyoto 606-8585, Japan

[2] Murata Manufacturing Co. Lt.
Tenjin, Nagaokakyo-shi, kyoto 617-8555, Japan

ABSTRACT

We have carried out direct numerical simulations for the motions of small heavy particles in a uniformly sheared turbulence. The effects of the inertia and the drift velocity of particles on their dispersion are examined systematically by changing these two parameters independently. It is found in the limit of zero particle inertia that the particle dispersion both in the streamwise and vertical directions becomes most active for the particles with some finite drift velocity. It is also found that the displacement of falling particles is asymmetric with respect to their mean displacement.

INTRODUCTION

The study of the dispersion of small heavy particles in turbulent flows is important for understanding many natural phenomena. An example is the dispersion of aerosol particles or ash from volcanic eruptions settling in the atmospheric turbulent boundary layer, which may have significant effects on the environment and the human health. In order to clarify the effects of the particle inertia and the particle drift velocity due to the gravitational force on the particle dispersion, the motion of heavy particles in a homogeneous isotropic turbulence has been extensively studied theoretically (Yudine, 1959, Csanady, 1963), experimentally (Snyder and Lumley, 1971, Wells and Stock, 1983) and numerically (Squires and Eaton, 1991b, Elghobashi and Truesdell, 1992). Yudine (1959) first recognized the crossing trajectories effect for particles settling under gravity; the dispersion of falling particles is small compared with that of the fluid particles. The motion of the particles in a uniformly sheared turbulence have been also studied as a first extension toward actual complex flows or as a typical example which exhibits anisotropy (Yeh and Lei, 1991, Liljegren, 1993, Simonin et al., 1995, Jiang et al., 1998). Yeh and Lei (1991) and Jiang et al. (1998) studied the dispersion of small heavy particles numerically. However, it has not yet been examined systematically how particle inertia and drift velocity affect the dispersion.

In the present study, the motion of heavy particles with various values of the particle inertia and drift velocity in a uniformly sheared turbulence are examined by the use of a direct numerical simulation (DNS). We particularly focus on the cases of small effect of inertia and noticeable effect of drift velocity, which are often encountered in the atmospheric boundary layer (Csanady, 1963).

FORMULATION

Fluid Motions

We consider the motion of small heavy spherical particles in homogeneous turbulence subjected to the mean flow in the x_1 direction that is uniformly sheared in the x_2 direction, $\overline{\boldsymbol{u}} = (\gamma x_2, 0, 0)$, where γ is the shear rate (see Fig.1). The equation for the fluctuating velocity, u_i', is written as

$$\frac{\partial u_i'}{\partial t} + \gamma x_2 \frac{\partial u_i'}{\partial x_1} + u_k \frac{\partial u_i'}{\partial x_k} = -\gamma u_2' \delta_{i1} - \frac{\partial p}{\partial x_i} + \nu \nabla^2 u_i' \quad (1)$$

with the solenoidal condition $\partial u_j'/\partial x_j = 0$, where p is the pressure and ν is the kinematic viscosity of the fluid.

Uniformly sheared turbulence is characterized by the Taylor microscale Reynolds number, R_λ, and the shear rate parameter, γ^*, which are respectively defined as

$$R_\lambda(t) \equiv \frac{u'\lambda}{\nu} = \left(\frac{L}{\eta}\right)^{\frac{2}{3}} = \frac{T}{\tau_\eta} = \left(\frac{u'}{v_\eta}\right)^2, \gamma^*(t) \equiv \gamma T. \quad (2)$$

Here, $\lambda = u'/\omega'$ denotes the Taylor microscale. $u'(= \overline{|\boldsymbol{u}'|})$ and $\omega'(= \overline{|\nabla \times \boldsymbol{u}'|})$ represent the magnitudes of

the fluctuating velocity and vorticity, respectively, and an overline denotes the spatial average. For $\omega' \gtrsim \gamma$, the smallest turbulent motions can be characterized by the Kolmogorov scales; $\eta = (\nu/\omega')^{1/2}$, $\tau_\eta = 1/\omega'$, and $v_\eta = \eta/\tau_\eta$, while the largest turbulent motions are represented by $L = u'^3/\epsilon$, $T = u'^2/\epsilon$, and u', where $\epsilon = \nu\omega'^2$ denotes the mean energy dissipation rate.

Particle Motions

The particle is assumed to be small enough, compared with the Kolmogorov length-scale of the turbulence. It is also assumed the concentration of particles is small enough such that the effect of the particles on the turbulence is negligible. Taking account of the fact that the particle (solid) density, ρ_p, is much larger than the fluid (air) density, ρ_f, only the Stokes drag and the gravitational forces are assumed to act on the particles (Maxey and Riley, 1983), i.e., the motion of the spherical particle with diameter, d_p, is assumed to follow

$$\frac{\mathrm{d}\boldsymbol{V}}{\mathrm{d}t} = \frac{1}{\tau_p}(\boldsymbol{u}(\boldsymbol{X}) - \boldsymbol{V} + \boldsymbol{V}_d), \quad \frac{\mathrm{d}\boldsymbol{X}}{\mathrm{d}t} = \boldsymbol{V}, \tag{3}$$

where $\boldsymbol{X}$ and $\boldsymbol{V}$ denote the position and the velocity of the particle, respectively, and

$$\boldsymbol{u}(\boldsymbol{X}) = \overline{\boldsymbol{u}}(\boldsymbol{X}) + \boldsymbol{u}'(\boldsymbol{X}) \tag{4}$$

is the total velocity of the surrounding fluid. τ_p $(= \rho_p d_p^2/18\rho_f\nu)$ represents the response time of the particle. $\boldsymbol{V}_d = \tau_p\boldsymbol{g} = (0, -v_d, 0)$ is the drift velocity of the particle due to the gravity, where $v_d = \tau_p g$ and $\boldsymbol{g} = (0, -g, 0)$ $(g > 0)$ denotes the gravity.

The particle inertia is expected to be effective when τ_p is larger than the smallest time-scale of turbulence τ_η, while the effect of the gravity becomes noticeable for the drift velocity higher than the lowest turbulent velocity v_η. For a sufficiently high drift velocity, the solid particle changes the velocity of its surrounding fluid more rapidly than the fluid particle, which leads to a decrease of the particle dispersion. This effect of particle drift is called crossing trajectories effect.

In order to extract the effects of the particle drift, it is helpful to consider the limiting case of zero particle inertia with the fixed drift velocity at a finite value. The particle velocity is expressed in this limit by the sum of the fluid velocity at the particle position and the drift velocity, that is,

$$\boldsymbol{V} = \boldsymbol{u}(\boldsymbol{X}) + \boldsymbol{V}_d \ \text{ or } \ \boldsymbol{V}' = \boldsymbol{u}'(\boldsymbol{X}) + \boldsymbol{V}_d \tag{5}$$

(Squire and Eaton, 1991b), where

$$\boldsymbol{V}' = \boldsymbol{V} - \overline{\boldsymbol{u}}(\boldsymbol{X}) \tag{6}$$

is the particle velocity relative to the mean shear flow. No preferential concentration of particles occurs in the case of zero particle inertia, and then the moments of the surrounding fluid velocity, $\boldsymbol{u}'(\boldsymbol{X})$, and those of the Eulerian fluid velocity, $\boldsymbol{u}'(\boldsymbol{x})$, coincide with each other, e.g.,

$$\left\langle u_i'(\boldsymbol{X})\right\rangle = \overline{u_i'} \ (= 0), \quad \left\langle u_i'(\boldsymbol{X})u_j'(\boldsymbol{X})\right\rangle = \overline{u_i'u_j'}. \tag{7}$$

Here, angle brackets, $\langle\ \rangle$, denote the ensemble average.

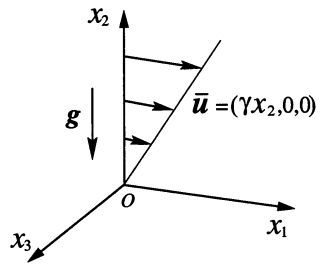

Figure 1. Uniform shear flow.

Displacement Tensor

For homogeneous turbulent shear flow, dispersion will depend on the initial vertical position of the particle, $X_2(t_0)$. Hence, we consider the displacement

$$Y_i(t) = X_i(t) - X_i(t_0) - \delta_{i2}\gamma(t - t_0)X_2(t_0) \tag{8}$$

for each particle, which corresponds to the shift of the origin of the coordinate to the initial position of each particle. In the present study, we focused on the displacement tensor of particles

$$Y_{ij} = \langle (Y_i - \langle Y_i\rangle)(Y_j - \langle Y_j\rangle)\rangle\,, \tag{9}$$

which represents the particle dispersion. For a stationary case, the displacement of (the same kind of) particles is simply expressed as

$$Y_1 - \langle Y_1\rangle = \int_{t_0}^{t} (V_1' - \left\langle V_1'\right\rangle + \gamma(Y_2 - \langle Y_2\rangle)\mathrm{d}\tau, \tag{10}$$

$$Y_i - \langle Y_i\rangle = \int_{t_0}^{t} (V_i' - \left\langle V_i'\right\rangle)\mathrm{d}\tau, \ (i = 2, 3), \tag{11}$$

where the mean particle velocity, $\langle V_i'\rangle$, is invariant in time and is given by

$$\begin{aligned} \left\langle V_1'\right\rangle &= \left\langle u_1'(\boldsymbol{X})\right\rangle - \gamma\tau_p(\left\langle u_2'(\boldsymbol{X})\right\rangle - v_d), \\ \left\langle V_2'\right\rangle &= \left\langle u_2'(\boldsymbol{X})\right\rangle - v_d, \ \left\langle V_3'\right\rangle = 0. \end{aligned} \tag{12}$$

The term $\gamma(Y_2 - \langle Y_2\rangle)$ in eq.(10) represents the effect of the mean shear and positive Y_{12} (Y_{22}) will amplify Y_{11} (Y_{12}) through this term.

Dispersion in Stationary Turbulence

For the stationary turbulence subjected to a uniform shear, the displacement tensor, Y_{ij}, of the *fluid* particles can be expressed in terms of the Lagrangian autocorrelation of fluctuating velocity, $\boldsymbol{u}'$ (see Monin and Yaglom, 1971). Based on eqs.(10) and (11), the formula can be extended to the solid particles as

$$\begin{aligned} Y_{11}(t) = &\frac{\gamma^2}{3}W_{22}\int_0^t (2t^3 - 3t^2\tau + \tau^3)R_{22}(0,\tau)\mathrm{d}\tau \\ &+\gamma W_{12}\int_0^t (t - \tau)^2 R_{21}(0,\tau)\mathrm{d}\tau \\ &+\gamma W_{12}\int_0^t (t^2 - \tau^2)R_{12}(0,\tau)\mathrm{d}\tau \end{aligned} \tag{13}$$

$$+2W_{11}\int_0^t (t-\tau)R_{11}(0,\tau)\mathrm{d}\tau$$

$$Y_{12}(t) = \gamma W_{12}\int_0^t t(t-\tau)R_{22}(0,\tau)\mathrm{d}\tau \quad (14)$$

$$+W_{12}\int_0^t (t-\tau)\{R_{12}(0,\tau)+R_{21}(0,\tau)\}\mathrm{d}\tau$$

$$Y_{22}(t) = 2W_{22}\int_0^t (t-\tau)R_{22}(0,\tau)\mathrm{d}\tau \quad (15)$$

$$Y_{33}(t) = 2W_{33}\int_0^t (t-\tau)R_{33}(0,\tau)\mathrm{d}\tau, \quad (16)$$

where R_{ij} is the Lagrangian autocorrelation tensor of fluctuating particle velocity which is defined as

$$R_{ij}(t_0,\tau) = \left\langle V_i''(t_0)V_j''(t_0+\tau)\right\rangle / W_{ij}. \quad (17)$$

Here,

$$V_i'' = V_i' - \left\langle V_i'\right\rangle. \quad (18)$$

The normalization factor was chosen as $W_{ij} = \left\langle V_i''(t_0)^2\right\rangle^{1/2}\left\langle V_j''(t_0+\tau)^2\right\rangle^{1/2}$, considering the application to non-stationary cases. Using the stationary condition, we put $t_0 = 0$ in eqs.(13)-(16). Since the normalization factors are positive, the cross components R_{21} and R_{12} take negative values if $\langle V_1''(t_0)V_2''(t_0)\rangle < 0$. For long travel times,

$$Y_{11}(t) \approx \frac{2}{3}\left\langle V_2''^2\right\rangle \gamma^2 T_{22}t^3, \quad Y_{12}(t) \approx \left\langle V_2''^2\right\rangle \gamma T_{22}t^2$$

$$Y_{22}(t) \approx \left\langle V_2''^2\right\rangle T_{22}t, \quad Y_{33}(t) \approx \left\langle V_3''^2\right\rangle T_{33}t, \quad (19)$$

where

$$T_{ii} = \int_0^\infty R_{ii}(0,\tau)\mathrm{d}\tau. \quad (20)$$

Note the relation for $\tau_p = 0$

$$\left\langle V_i''V_j''\right\rangle = \overline{u_i'u_j'} \quad (21)$$

which is obtained from eqs.(5),(7) and (12). It should also be noted that the relations (13)-(16) are exact only for stationary homogeneous turbulence. Actually, the length scales and the turbulence energy will continue to grow in time in uniformly sheared turbulence.

Numerical Method

Navier-Stokes equations were solved on 160^3 grid points in a rectangular box of sides $4\pi \times 2\pi \times 2\pi$, by using the Fourier spectral/ Runge-Kutta-Gill scheme, starting with random and isotropic initial conditions. The initial conditions were similar to those in Kida and Tanaka (1994), but resolutions for both small and large scales were improved by increasing the number of the grid points. As was reported in Kida and Tanaka (1994), the turbulence energy increased exponentially in time, while the turbulence attained a statistically quasi-equilibrium state where the second order moments of the velocity developed similarly.

Twelve types of particles with different values of inertia and drift velocity, $\tau_p/\tau_\eta(0) = 0, 0.25$ and $v_d/v_\eta(0) = 0, 1, 2, 4, 8, 16$, were considered in this study. For each combination of τ_p and v_d, we introduced $32768(= 32^3)$ particles randomly throughout the computational domain at the non-dimensional time of $\gamma t = 3$. The reference time was set to $\gamma t_0 = 4$ when the particles with inertia had fully responded to the fluid ($\gamma\tau_p = 0.25$) and the turbulence had attained the quasi-equilibrium state. Equations (3) were integrated for each particle with inertia until $\gamma t = 16$, using Runge-Kutta-Gill scheme with the initial condition $\boldsymbol{V}(t_0) = \boldsymbol{u}(\boldsymbol{X}(t_0))$. Equations (4) and $\mathrm{d}\boldsymbol{X}/\mathrm{d}t = \boldsymbol{V}$ were solved in the same manner for the case of zero particle inertia. The 13-point spatial interpolation method (Yeung and Pope, 1988) was used to evaluate the fluid velocity at the particle position from its neighboring grid points.

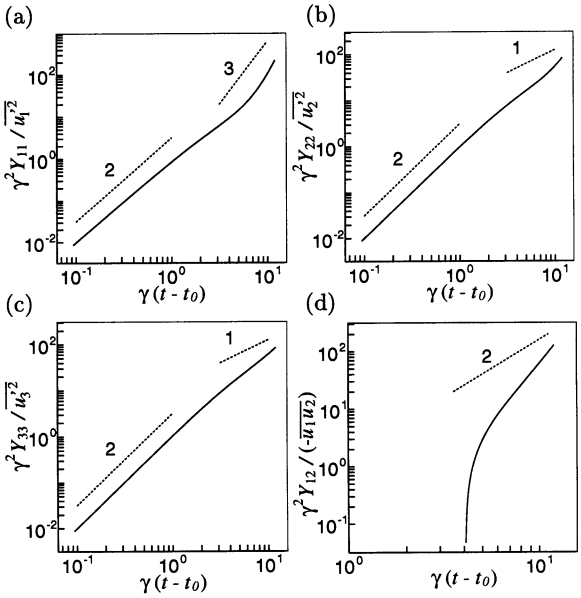

Figure 2. Time evolution of the displacement tensor. (a) Y_{11}, (b) Y_{22}, (c) Y_{33}, (d) Y_{12}. $\overline{u_1'^2}/\gamma^2 = 0.0119$, $\overline{u_2'^2}/\gamma^2 = 0.0027$, $\overline{u_3'^2}/\gamma^2 = 0.0060$, $-\overline{u_1'u_2'}/\gamma^2 = 0.0036$.

The ratio of the largest length scale of turbulence to the length of the computational box in the x_1 direction, $L/4\pi$, varied from 0.138 at $\gamma t = 4$ to 0.375 at $\gamma t = 16$. $k_{max}\eta$ ($k_{max} = 80$) was 1.85 at $\gamma t = 4$ and 1.16 at $\gamma t = 16$. The time increment was set to be less than 1/10 of τ_p, and the Courant number varied from 0.25 at $\gamma t = 4$ to 0.67 at $\gamma t = 16$. The shear rate parameter, γ^*, stayed in the range of $12 \sim 14$ after $\gamma t = 4$, while the Reynolds number, R_λ, increased from 17.8 at $\gamma t = 4$ to 47.2 at $\gamma t = 16$.

Finally, we note that Kolmogorov scales, τ_η and v_η also varied in time and that $\tau_p/\tau_\eta(t)$ and $v_d/v_\eta(t)$ changed by factors of 3.72 and 0.52, respectively, at the end of the simulation.

RESULTS

Dispersion of Fluid Particles

First, we discuss the dispersion of fluid particles

briefly. Figure 2 shows the time evolution of non-zero components of the displacement tensor normalized by the shear rate and the corresponding rms velocity at the reference time $\gamma t_0 = 4$. Figures 2(a)-2(c) show that the short-time behavior of the dispersion is proportional to t^2, which agrees with the theoretical prediction from eqs.(11)-(14) that $Y_{ii} = \overline{u_i' u_i'}(t_0)(t - t_0)^2$ for $t - t_0 \ll 1$. Since $Y_{12} = \overline{u_1' u_2'}(t_0)(t - t_0)^2 < 0$ at an initial period, only the time evolution in a later period is shown in Fig.2(d). The long-time behavior of Y_{ij} is quite different from the asymptotic formula of eqs.(16). The slopes become steeper than those predicted by eqs.(16) owing to the increase of turbulence energy, which was also found in Squire and Eaton (1991a), Yeh and Lei (1991) and Shen and Yeung (1997).

Effects of Particle Drift

For particles with small inertia, the particle dispersion, Y_{ij}, varies in a highly anisotropic manner by increasing the drift velocity, v_d. Figure 3 shows the time evolution of Y_{ij} for the limiting case that $\tau_p = 0$. They were normalized by the corresponding values for the fluid particles to emphasize the modulation due to the effect of particle drift. The drift velocity are increasing from Line A to Line F.

It is observed from Fig.3(c) that the dispersion in the x_3-direction, Y_{33}, decreases with an increasing of the drift velocity due to the crossing trajectories effect. At large values of v_d, doubling of the drift velocity (e.g. Line F against Line E) almost leads to the reduction by half of the dispersion in agreement with the asymptotic behavior, $Y_{33} \propto v_d^{-1}$, for $v_d \gg u'$ (Csanady, 1963).

The dispersion in the x_2 directions, Y_{22}, also decreases initially with an increase of the drift velocity. In the later period, however, it increases from that in the case of $v_d = 0$ as the drift velocity increases, takes maximum at $v_d/v_\eta(0) = 4$ (Line D) and decreases with further increase of v_d. It should be noted that the magnitude of vertical fluctuating velocity, u_2', is $1.87 \sim 5.73$ times larger than $v_\eta(0)$ and comparable with the value of $v_d (\approx 4v_\eta(0))$ at which the dispersion is the most activated.

The dispersion in the x_1 direction, Y_{11}, evolves in a similar way as Y_{22}. Though the relative magnitude Y_{11}(solid particle)/Y_{11}(fluid particle) may behave as T_{22}(solid particle)/T_{22}(fluid particle) $\approx Y_{22}$(solid particle)/Y_{22}(fluid particle) for sufficiently large values of t as is predicted from eqs.(19) and (21), the enhancement of the particle dispersion is much more noticeable for Y_{11} than Y_{22} at $\gamma(t - t_0) \approx 10$.

As mentioned above, Y_{12} is initially negative, and then becomes positive in a later period. The time at which it becomes positive is earlier for larger values of the drift velocity. This is a direct consequence of the reduction in Lagrangian velocity autocorrelation due to the effect of the drift (see below). In the later period, the maximum enhancement of Y_{12} is achieved at $v_d/v_\eta(0) = 4$ as Y_{11} and Y_{22}.

Effects of Particle Inertia

Figure 4 shows the time evolution of Y_{ij} for the particles with finite inertia ($\tau_p/\tau_\eta(0) = 0.25$). As in Figs.3(a)-3(d), it is normalized by the value for the fluid particles. The values of Y_{ii} at $t = t_0$ shown in

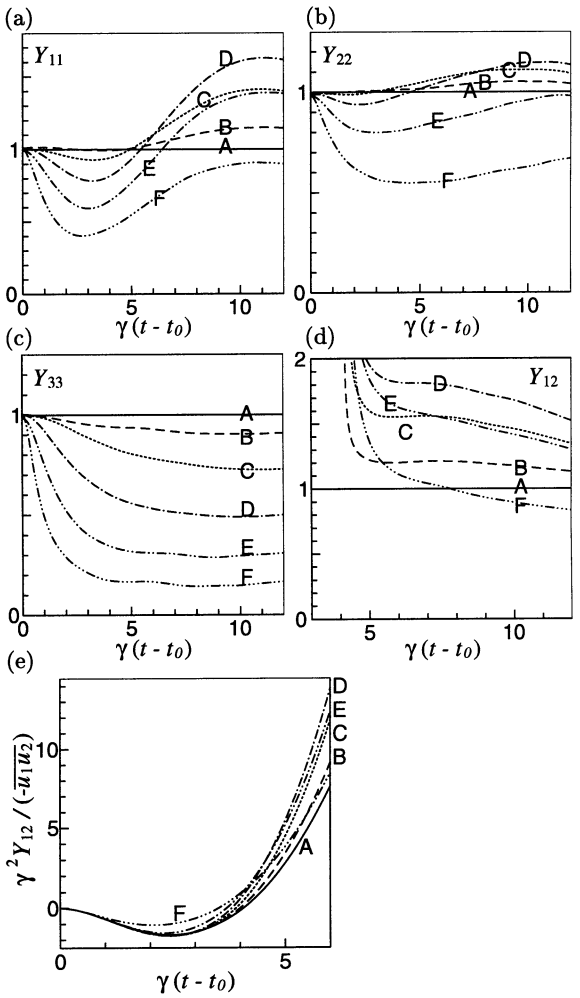

Figure 3. Time evolution of the displacement tensor for $\tau_p = 0$. (a) Y_{11}, (b) Y_{22}, (c) Y_{33}, (d),(e) Y_{12}. A: $v_d/v_\eta(0) = 0$ (fluid particle), B: $v_d/v_\eta(0) = 1$, C: $v_d/v_\eta(0) = 2$, D: $v_d/v_\eta(0) = 4$, E: $v_d/v_\eta(0) = 8$, F: $v_d/v_\eta(0) = 16$. $\gamma t_0 = 4$.

Figs.4(a)-(c) represent the relative magnitude of the fluctuating particle velocity $\langle V_i'' V_i'' \rangle / \overline{u_i' u_i'}$. In the absence of the gravity (see Lines A), it is found that the initial dispersion ($\propto \langle V_i'' V_i'' \rangle (t - t_0)^2$) is enhanced for the streamwise component, but is reduced for both vertical and spanwise components by the effect of particle inertia. The relative dispersion increases later except the streamwise component which shows a temporary decrease. The increase of Y_{33} due to the effect of particle inertia was also found in Yeh and Lei (1991).

The increases in Y_{11}, Y_{22} and Y_{12} due to the effect of particle drift, which was observed for $\tau_p = 0$, are also found for the particles with inertia. However, Y_{22} for the particles with $v_d/v_\eta(0) = 4$ (Line D) is less than that for the particles with $v_d = 0$ (Line A) as opposed to the case of $\tau_p = 0$. On the other hand, Y_{11} and Y_{12} for the former (Line D) are still larger than those for the latter (Line A) at this value of particle inertia.

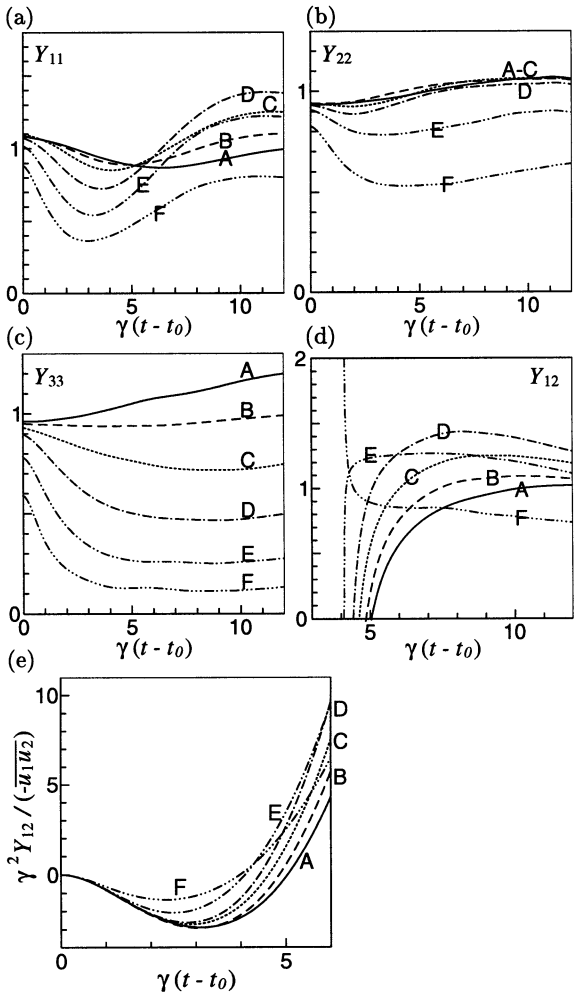

Figure 4. The same as figure 3 but for $\tau_p/\tau_\eta(0) = 0.25$.

Finally, we note that the average settling velocity, $|\langle V_2 \rangle|$, is greater than the drift velocity (not shown) as in isotropic turbulence (Wang and Maxey, 1993).

Lagrangian Velocity Autocorrelation

Although the relations in eqs.(13)-(16) are not exact for the non-stationary turbulence studied here, the Lagrangian velocity autocorrelation is found to provide useful information for the understanding of dispersion phenomena. In Fig. 5, the Lagrangian velocity autocorrelation is shown for the fluid particles (solid lines) and for the solid particles with $\tau_p = 0$ and $v_d/v_\eta(0) = 4$ (broken lines) which correspond to Lines D in Fig.(3). In Fig.5(d), R_{21} and R_{12} are denoted by the thick and thin lines, respectively. For the fluid particles the correlation is the strongest in the x_1 direction and is the weakest in the x_2 direction. It is interesting that the correlation in the x_2 direction takes negative values around $\gamma(t - t_0) = 4.5$ (Squires and Eaton, 1991a).

It is seen from Fig.5(a) that the correlation of the streamwise velocity component is significantly reduced due to the effect of particle drift, though this decrease

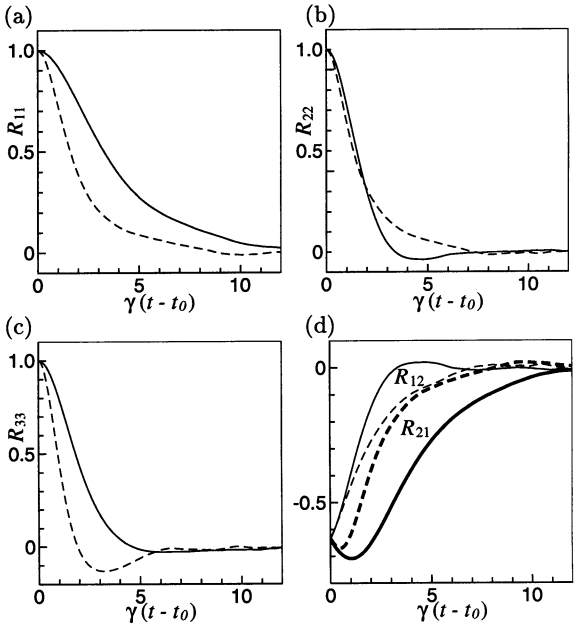

Figure 5. Lagrangian velocity autocorrelation function. (a) R_{11}, (b) R_{22}, (c) R_{33}, (d) R_{21}, R_{12}. $\gamma t_0 = 4$.

in R_{11} may be irrelevant to the long-time behavior of the streamwise component of dispersion (see eq.(13)). The other transverse component, R_{33}, also decreases due to the particle drift. The negative region found at $\gamma(t-t_0) \approx 3$ is characteristic of the crossing trajectories effects, which was also found in an isotropic turbulence (Squires and Eaton, 1991b).

The vertical component, R_{22}, for the solid particles decreases rapidly in an initial period compared with that for the fluid particles. In the later period, however, it decreases more slowly than that for the fluid particles. The increase of Y_{22} due to the particle drift shown in Fig.3(b) may be caused by this slow decay of the correlation.

It is seen from Fig.5(d) that the particle drift increases R_{21} and decreases R_{12}. The increase of R_{21} is found to be much larger than the decrease of R_{12}. This may be considered the main reason for the enhancement of Y_{11} due to the effect of particle drift (see Fig.3(a)), because the suppression of Y_{11} which is caused by the second term on the rhs of eq.(13) is weakened by the increase of R_{21}. A continuous stay of particles in a region of negative $u_1' u_2'$ will suppress the growth of Y_{11}, however falling particles can be suspended in a region of $u_1' u_2' < 0$ for a shorter duration compared with fluid particles.

For the case without gravity, the particle inertia makes the correlation stronger except for the streamwise component, R_{11} (figure omitted). The increases of Y_{22} and Y_{33}, and the initial decrease of Y_{12} compared with the fluid particles may be attributed to this increase of the correlation.

Asymmetry of Particle Displacement

Figure 6 shows the time evolution of the skewness

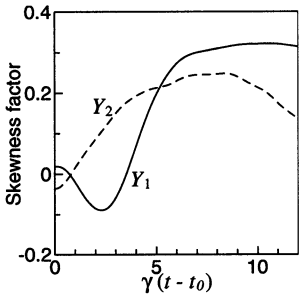

Figure 6. Skewness factors of Y_{11} and Y_{22}.

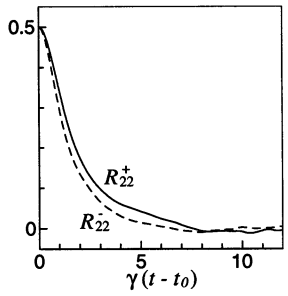

Figure 7. Contribution to R_{22} from particles with $u_2(\boldsymbol{X}(t_0)) > 0$ ($R_{22}{}^+$) and $u_2(\boldsymbol{X}(t_0)) < 0$ ($R_{22}{}^-$) .

factors of Y_{11} and Y_{22} for the particles with $\tau_p = 0$ and $v_d/v_\eta(0) = 4$. The skewness of Y_{22} increases initially, takes the value about 0.2, and decreases gradually in the later period. The skewness of Y_{11} initially takes negative values, and then increases up to about 0.3. It can be seen that the skewness of Y_{11} reflects that of Y_{22} and the sign of the correlation between Y_1 and Y_2 (Y_{12}).

This asymmetry of particle displacement may be related with the fact that a particle trapped in a region of $u_2' > 0$ tend to stay there for a longer time than that in a region of $u_2' < 0$. Figure 7 shows the contributions to the Lagrangian velocity autocorrelation, R_{22}, from the solid particles which were initially located in the regions of $u_2' > 0$ ($R_{22}{}^+$, solid line) and $u_2' < 0$ ($R_{22}{}^-$, broken line). It is seen from the figure that the correlation drops more slowly for the particles which were initially located in up-flow regions than those in down-flow regions, which may lead to the skew of Y_{22}.

CONCLUSION

We have carried out DNS for the dispersion of small heavy particles in a uniformly sheared turbulence. It is found for particles with small inertia that the particle dispersion, Y_{ij}, varies in a highly anisotropic manner by increasing the drift velocity. The particle dispersion in the spanwise (x_3) direction decreases monotonously with increasing drift velocity due to the crossing trajectories effect, while the dispersion both in the streamwise (x_1) and vertical (x_2) directions is most activated at some finite drift velocity close to the vertical fluctuating velocity u_2'. The enhancement of the particle dispersion is much more noticeable for Y_{11} than Y_{22} at intermediate times, since the cross component of the Lagrangian velocity autocorrelation R_{21}, which plays a role to suppress the growth of Y_{11}, is weakened by the effect of the particle drift. For $\tau_p \ll \tau_\eta$, the displacement of falling particles is asymmetric with respect to its mean value, which can be associated with the tendency that particles stay in a region of $u_2' > 0$ for a longer time than in a region of $u_2' < 0$.

REFERENCES

Csanady, G.T., 1963, "Turbulent diffusion of heavy particles in the atmosphere," J. Atmos. Sci., Vol.20, pp.201-208.

Elghobashi, S. and Truesdell, G.C., 1992, "Direct simulation of particle dispersion in a decaying isotropic turbulence," J. Fluid Mech., Vol.242, pp.655-700.

Jiang, Y., Huang, X. and Stock, D.E., 1998, "Using random Fourier modes to simulate particle dispersion in a uniform shear flow," CD-ROM containing the Proc. of the Third International Conference on Multiphase Flow, ICMF'98, Lyon, France, June, 1998.

Kida, S. and Tanaka, M., 1994, "Dynamics of vortical structures in a homogeneous shear flow," J. Fluid Mech., Vol.274, pp.43-68.

Liljegren, L.M., 1993, "The effect of a mean fluid velocity gradient on the streamwise velocity variance of a particle suspended in a turbulent flow," Int. J. Multiphase Flow, Vol.19, pp.471-484.

Maxey, M.R. and Riley, J.J, 1983, "Equation of motion for a small rigid sphere in a nonuniform flow," Phys. Fluids, Vol.26, pp.883-889.

Monin, A.S. and Yaglom, A.M., 1971, Statistical Fluid Mechanics, edited by J.L. Lumley (MIT press, Cambridge, MA).

Simonin, O., Deutsch, E. and Bovin, M., 1995, "Large eddy simulation and second-moment closure model of particle fluctuating motion in two-phase turbulent shear flows.," Turbulent Shear Flows 9, pp.85-115.

Squires, K.D. and Eaton, J.K., 1991a, "Lagrangian and Eulerian statistics obtained from direct numerical simulations of homogeneous turbulence," Phys. Fluids A, Vol.3, pp.130-143.

Squires, K.D. and Eaton, J.K., 1991b, "Measurements of particle dispersion obtained from direct numerical simulations of isotropic turbulence," J. Fluid Mech. Vol.226, pp.1-35.

Snyder, W.H. and Lumley, J.L., 1971, "Some measurements of particle velocity autocorrelation functions in a turbulent flow", J. Fluid Mech. Vol.48, pp.41-71.

Wang, L.P. and Maxey, M.R., 1993, "Settling velocity and concentration distribution of heavy particles in homogeneous isotropic turbulence," J. Fluid Mech. Vol.256 pp.27-68.

Wells, M.R. and Stock, D.E., 1983, "The effects of crossing trajectories on the dispersion of particles in a turbulent flow", J. Fluid Mech. Vol.136, pp.31-62.

Yeh, F. and Lei, U, 1991, "On the motion of small particles in a homogeneous turbulent shear flow," Phys. Fluids A, Vol.3, pp.2758-2776.

Yeung, P.K. and Pope, S.B., 1988, "An algorithm for tracking fluid particles in numerical simulations of homogeneous turbulence," J. Comp. Phys., Vol.79, pp.373-416.

Yudine, M.I., 1959, "Physical consideration on heavy-particle dispersion," Adv. Geophys, Vol. 6, pp.185-191.